

problem in V and $S_h \subset V$ by u and u_h , respectively. Then, there exists $C > 0$ such that we have the following inequality

$$\|u - u_h\|_1 \leq \frac{C}{\alpha} \inf_{v_h \in S_h} \|u - v_h\|_1 .$$

Proof: We have

$$\begin{aligned} a(u, v) &= (f, v)_0 \quad \forall v \in V \\ a(u_h, v_h) &= (f, v_h)_0 \quad \forall v_h \in S_h , \end{aligned}$$

which implies the so-called *Galerkin orthogonality*

$$a(u - u_h, v_h) = 0 \quad \forall v_h \in S_h .$$

Let $v_h \in S_h$, so that with $w_h := v_h - u_h \in S_h$ we obtain

$$a(u - u_h, v_h - u_h) = 0$$

and by coercivity and boundedness

$$\begin{aligned} \alpha \|u - u_h\|_1^2 &\leq a(u - u_h, u - u_h) \\ &= a(u - u_h, u - v_h) + \underbrace{a(u - u_h, v_h - u_h)}_{=0} \\ &\leq C \|u - u_h\|_1 \|u - v_h\|_1 \end{aligned}$$

which proves the theorem. \square

Sometimes this method is also simply called *Galerkin method* and the solution $u_h \in S_h$ is called the *Galerkin solution* or *Galerkin approximation*. The finite dimensional space S_h is also called *trial space*.

6.5 Some Simple Finite Elements

Again, we consider the homogeneous model problem

$$-\Delta u = f \quad \text{in } \Omega, \quad u = 0 \quad \text{on } \partial\Omega$$

where $\Omega = (0, 1)^2$. The idea is to subdivide Ω into regular triangles of meshsize h as indicated in Figure 6.3. Using this *triangulation* of Ω , we define the trial space

$$S_h := \{v \in C(\bar{\Omega}) : v \text{ is linear in each triangle and } v|_{\partial\Omega} = 0\} .$$

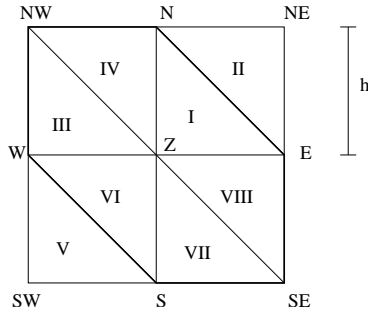


Figure 6.3: Support of the Courant Finite Element.

In each triangle (*element*) a $v_h \in S_h$ takes the form

$$v_h(x, y) = a + bx + cy, \quad a, b, c \in \mathbb{R},$$

i.e., v_h is uniquely determined by the value at three different nodes. From this we can easily see that

$$N = \dim S_h = \text{number of interior grid points}$$

and $v_h \in S_h$ is globally (i.e., on $\bar{\Omega}$) determined by its values on these N grid points. The canonical (so-called *nodal*) basis $\{\psi_i\}_{i=1, \dots, N}$ is defined by

$$\psi_i(x_j, y_j) = \delta_{ij}.$$

In Figure 6.3, the support of ψ_Z is shown. Let h denote the mesh size of the triangles, then we obtain the following values for the derivatives of ψ_Z (see Figure 6.3).

triangle	I	II	III	IV	V	VI	VII	VIII
$\partial_x \psi_Z$	$-h^{-1}$	0	h^{-1}	0	0	h^{-1}	0	$-h^{-1}$
$\partial_y \psi_Z$	$-h^{-1}$	0	0	$-h^{-1}$	0	h^{-1}	h^{-1}	0

Then, straightforward calculations show that by symmetry we have

$$\begin{aligned}
a(\psi_Z, \psi_Z) &= \int_{\text{I-VIII}} (\nabla \psi_Z)^2 dx dy \\
&= 2 \int_{\text{I} \cup \text{III} \cup \text{IV}} [(\partial_x \psi_Z)^2 + (\partial_y \psi_Z)^2] dx dy \\
&= 2h^{-2} \left\{ \underbrace{\int_{\text{I} \cup \text{III}} dx dy}_{=h^2} + \underbrace{\int_{\text{IV}} dx dy}_{=h^2} \right\} \\
&= 4
\end{aligned}$$

for the diagonal entries of the stiffness matrix and

$$\begin{aligned}
a(\psi_Z, \psi_N) &= \int_{\text{I} \cup \text{IV}} \nabla \psi_Z \cdot \nabla \psi_N dx dy \\
&= \int_{\text{I} \cup \text{IV}} (\underbrace{\partial_x \psi_Z \partial_x \psi_N}_{=0} + \partial_y \psi_Z \partial_y \psi_N) dx dy \\
&= -h^{-2} \int_{\text{I} \cup \text{IV}} dx dy \\
&\quad \underbrace{\hspace{10em}}_{=h^2} \\
&= -1 = a(\psi_Z, \psi_O) \\
&= a(\psi_Z, \psi_S) = a(\psi_Z, \psi_W).
\end{aligned}$$

Finally, we obtain

$$\begin{aligned}
a(\psi_Z, \psi_{NW}) &= \int_{\text{III} \cup \text{IV}} (\partial_x \psi_Z \partial_x \psi_{NW} + \partial_y \psi_Z \partial_y \psi_{NW}) dx dy \\
&= \int_{\text{III}} h^{-1} \cdot 0 + 0 \cdot h^{-1} + \int_{\text{IV}} 0 \cdot (h^{-1}) + (-h^{-1})0 = 0
\end{aligned}$$

and again by symmetry

$$a(\psi_Z, \psi_{SO}) = a(\psi_Z, \psi_{SW}) = a(\psi_Z, \psi_{NO}).$$

This means that in this particular case of a uniform triangulation and the nodal basis for piecewise linear finite elements the stiffness matrix coincides with the matrix arising from the 5-point-stencil in finite difference methods. This principle, however, is not true in general, i.e., for a finite element discretization there is in general *not* an equivalent finite difference discretization. Finite elements are much more flexible than finite differences and they allow the treatment of the weak formulation of the bvp.

Some properties of finite elements

- 1.) Subdivision (or *partition*) of Ω in triangular or quadrilateral elements. If all elements are congruent, this is called a *regular* subdivision.
- 2.) In 2D, we denote by

$$\mathcal{P}_t := \left\{ u(x, y) = \sum_{i+k \leq t; i, k \geq 0} c_{i,k} x^i y^k \right\}$$

the set of all algebraic polynomials of degree at most t . The restriction of the trial (or *shape*) functions to an element is a polynomial.

- 3.) Smoothness: A finite element is said to be *of order* k if it is in $C^k(\Omega)$.

For the example of the *Courant Finite Element* which is shown in Figure 6.3, we have $t = 1$ and $k = 0$.

Definition 6.5.1 (i) A partition $\mathcal{T} = \{T_1, \dots, T_M\}$ of Ω in triangular or quadrilateral elements is called *admissible*, if

- a) $\bar{\Omega} = \bigcup_{i=1}^M T_i$
- b) If $T_i \cap T_j$ consists of exactly one point, this point is a corner of both T_i and T_j .
- c) If $T_i \cap T_j$, $i \neq j$ consists of more than one point, then $T_i \cap T_j$ is a common edge of T_i and T_j .

(ii) We write \mathcal{T}_h if each element has a diameter of at most $2h$.

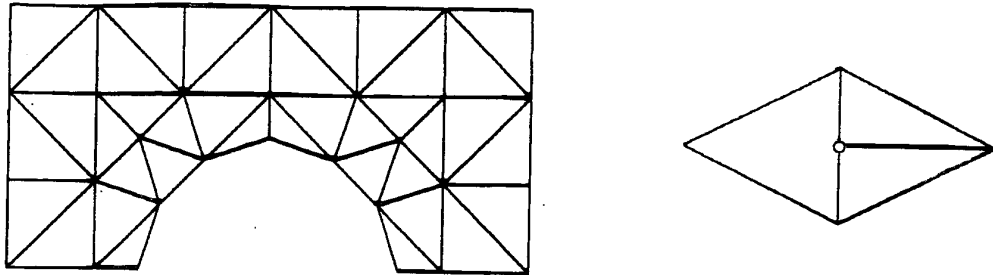


Figure 6.4: An admissible triangulation (left) and a non-admissible triangulation (right) with a hanging node. (Taken from [1].)

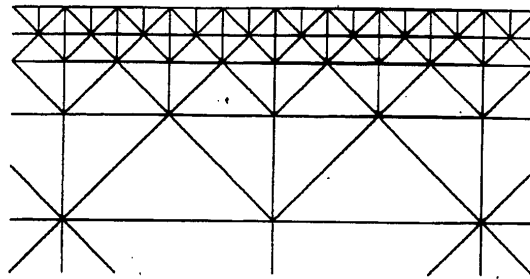


Figure 6.5: A quasi-uniform but non-uniform triangulation. (Taken from [1].)

(iii) \mathcal{T}_h is called quasi-uniform if there exists some $\kappa > 0$ such that each $T \in \mathcal{T}_h$ contains a circle with radius

$$\rho_T \geq \frac{h_T}{\kappa}.$$

Examples of triangulations are shown in Figures 6.4-6.6.

The following theorem shows how to choose the order of the elements in order to be contained in a certain Sobolev space. If the finite elements are contained in the Sobolev space corresponding to the variational formulation, the elements are called *conforming*, otherwise *non-conforming*. For the elliptic second order problem this would mean that the elements are conforming if $S_h \subset H_0^1(\Omega)$.

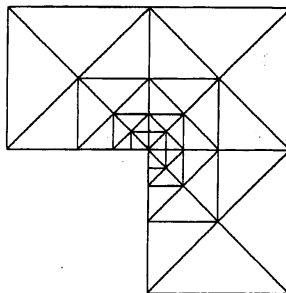


Figure 6.6: A non-uniform triangulation at a reentrant corner. (Taken from [1].)

Theorem 6.5.2 *Let $k \geq 1$ and Ω be bounded. A piecewise C^∞ -function $v : \bar{\Omega} \rightarrow \mathbb{R}$ is in $H^k(\Omega)$ if and only if $v \in C^{k-1}(\bar{\Omega})$. \square*

The latter theorem in particular implies that for the elliptic second order problem we would have $k = 1$ thus $v \in C^0(\bar{\Omega})$ which in particular shows that the Courant Finite Element is conforming.

Definition 6.5.3 *For any finite element space there is a set of points in the sense that the shape functions are uniquely defined by the values at these points. Those functions that take the value 1 at exactly one of these points and 0 on all the others are called nodal basis functions or Lagrange elements.*

Table 6.1 shows a number of standard finite elements. We also show some higher order elements in which the point values are not sufficient to define a shape function uniquely. Also certain derivatives are needed in that case.

Remark 6.5.4 *With the aid of affine mappings, one can usually reduce oneself to one single reference element T_{ref} , i.e., for any $T_j \in \mathcal{T}$ there exists an affine mapping $F_j : T_{\text{ref}} \rightarrow T_j$ such that*

$$v_h(x)|_{T_j} = p(F_j^{-1}x)|_{T_j}, \quad p \in \mathcal{P}_{\text{ref}}, \quad v_h \in S_h.$$

6.6 Approximation Results

In this section, we give some results concerning the approximation properties of the finite element method and also derive some error estimates.

- value of the function
- ⊙ value of the function, 1st and 2nd derivative
- ⊥ normal derivative

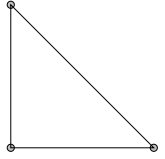
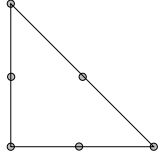
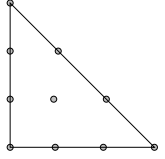
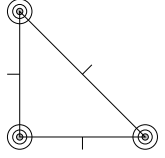
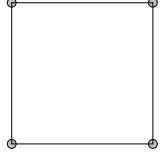
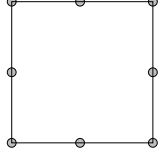
	<p>Linear triangular element</p> <p>$u \in C^0(\Omega)$</p> <p>$\Pi_{\text{ref}} = \mathcal{P}_1, \dim \Pi_{\text{ref}} = 3$</p>
	<p>Quadratic triangular element</p> <p>$u \in C^0(\Omega)$</p> <p>$\Pi_{\text{ref}} = \mathcal{P}_2, \dim \Pi_{\text{ref}} = 6$</p>
	<p>Cubic triangular element</p> <p>$u \in C^0(\Omega)$</p> <p>$\Pi_{\text{ref}} = \mathcal{P}_3, \dim \Pi_{\text{ref}} = 10$</p>
	<p>Agyris element</p> <p>$u \in C^1(\Omega)$</p> <p>$\Pi_{\text{ref}} = \mathcal{P}_5, \dim \Pi_{\text{ref}} = 21$</p>
	<p>Linear quadrilateral element</p> <p>$u \in C^0(\Omega)$</p> <p>$\Pi_{\text{ref}} = \mathcal{P}_2, u _{\partial T_i} \in \mathcal{P}_1, \dim \Pi_{\text{ref}} = 4$</p>
	<p>Quadrilateral serendipity element</p> <p>$u \in C^1(\Omega)$</p> <p>$\Pi_{\text{ref}} = \mathcal{P}_3, u _{\partial T_i} \in \mathcal{P}_2, \dim \Pi_{\text{ref}} = 8$</p>

Table 6.1: Standard Finite Elements. (Taken from [1].)

Definition 6.6.1 For any partition $\mathcal{T}_h = \{T_1, \dots, T_M\}$ of Ω and $m \geq 1$, we define the grid norm by

$$\|v\|_{m,h} := \left(\sum_{T_j \in \mathcal{T}_h} \|v\|_{m,T_j}^2 \right)^{1/2}.$$

Obviously, we have $\|v\|_{m,h} = \|v\|_{m,\Omega}$ for $v \in H^m(\Omega)$.

The following well-known theorem is a central statement in functional analysis.

Theorem 6.6.2 (Bramble-Hilbert theorem) Let $\Omega \subset \mathbb{R}^2$ be a domain with Lipschitz-continuous boundary, $t \geq 2$ and let $L : H^t(\Omega) \rightarrow Y$ be a linear, bounded operator on a normed space Y . If $\mathcal{P}_{t-1}(\Omega) \subset \text{Ker}(L)$, then we have

$$\|Lv\|_Y \leq c |v|_t$$

for all $v \in H^t(\Omega)$ with a constant $c = c(L, \Omega)$. \square

We now apply this theorem to the interpolation operator

$$I_h : H^t(\Omega) \rightarrow S_h,$$

which is defined by interpolation of the input function with respect to the nodal grid points of the underlying triangulation. Then, we immediately obtain the following error estimate.

Theorem 6.6.3 Let $t \geq 2$ and \mathcal{T}_h be a quasi-uniform triangulation of Ω . Then, we have for the interpolation operator I_h defined by interpolation with piecewise polynomials of degree $t - 1$ that

$$\|u - I_h u\|_{m,h} \leq ch^{t-m} |u|_{t,\Omega}$$

for $u \in H^t(\Omega)$, $0 \leq m \leq t$ and some constant $c = c(\Omega, \mathcal{T}_h, t)$. \square

The principle behind the latter theorem can be roughly described as ‘polynomial exactness implies approximation power’. This is also known as *Bramble-Hilbert type argument*.

Finally, we give an *a priori* error estimate which also shows the continuous dependence of the error on the right-hand side data.

Theorem 6.6.4 *Let \mathcal{T}_h be a family of quasi-uniform triangulations of a convex domain Ω . Then, the piecewise linear finite element approximation $u_h \in S_h$ satisfies the following estimate*

$$\|u - u_h\|_1 \leq ch\|u\|_2 \leq ch\|f\|_0 . \quad \square$$

Remark 6.6.5 (i) *The above regularity assumption $u \in H^2(\Omega)$ can also be weakened.*

(ii) *The computation of an appropriate triangulation is a problem on its own, in particular for complex geometries Ω .*

(iii) *The setup of the linear system (stiffness matrix and right-hand side) is usually done on the reference element.*

6.7 Example: 1D Finite Element Discretization for the Black-Scholes Equation

A variational formulation in 1D reads $a(u, v) = (f, v)_0$ for all $v \in H_0^1(\Omega)$, where $\Omega = (0, 1)$ and (e.g.)

$$a(u, v) = (u', v')_{0,(0,1)} + (u', v)_{0,(0,1)} + (u, v)_{0,(0,1)}.$$

We now subdivide $(0, 1)$ uniformly by equidistant grid points $x_h^k := kh$, where $h = \frac{1}{M}$, $k = 0, \dots, M$, i.e., we have $M - 1$ interior nodes. An ‘element’ in 1D is hence a subinterval (x_h^{k-1}, x_h^k) , $k = 1, \dots, M$. Next, we consider the nodal basis as shown in Figure 6.7. We now apply this for the Black-Scholes equation for european option pricing

$$\frac{\partial}{\partial t} u(t, x) + \frac{1}{2} \sigma^2 x^2 \frac{\partial^2}{\partial x^2} u(t, x) + rx \frac{\partial}{\partial x} u(t, x) - ru(t, x) = 0,$$

where u is the value of the option, x is the asset price, r is the interest rate and σ is the volatility. We consider the call, i.e., the terminal condition

$$u(T, x) = \max(K - x, 0),$$

where again K denotes the strike. We rewrite this in coefficient form

$$\frac{\partial}{\partial t} u(t, x) + \frac{\partial}{\partial x} \left(c(x) \frac{\partial}{\partial x} u(t, x) \right) + b(x) \frac{\partial}{\partial x} u(t, x) - ru(t, x) + ad_a u(t, x) = 0,$$

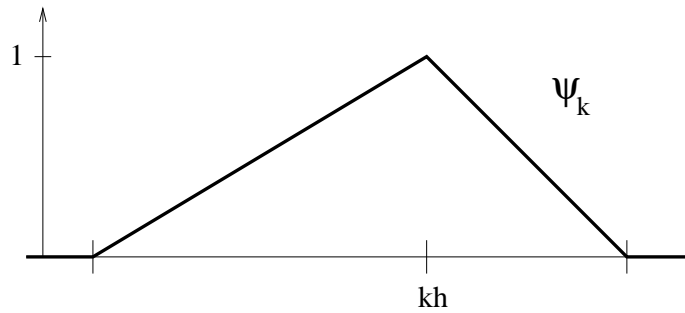


Figure 6.7: 1D nodal piecewise linear shape function.

which is required for FEMLAB

$$\frac{\partial}{\partial t}u(t, x) + \frac{\partial}{\partial x} \left(\frac{1}{2}\sigma^2 x^2 \frac{\partial}{\partial x} u(t, x) \right) + \left(rx - \frac{\partial}{\partial x} \left(\frac{1}{2}\sigma^2 x^2 \right) \right) \frac{\partial}{\partial x} u(t, x) - ru(t, x) = 0,$$

i.e.,

$$\begin{aligned} c &:= \frac{1}{2}\sigma^2 x^2 \\ b &:= (r - \sigma^2)x = rx - \frac{\partial}{\partial x} \left(\frac{1}{2}\sigma^2 x^2 \right) \\ a &:= r, \\ d_a &:= -1. \end{aligned}$$

In this form, we can immediately solve this equation in FEMLAB and we show the computed solution for $K = 40$, $\sigma = 0.3$, $r = 0.12$, $x = 80$ and $T = 12$ in Figure 6.8.

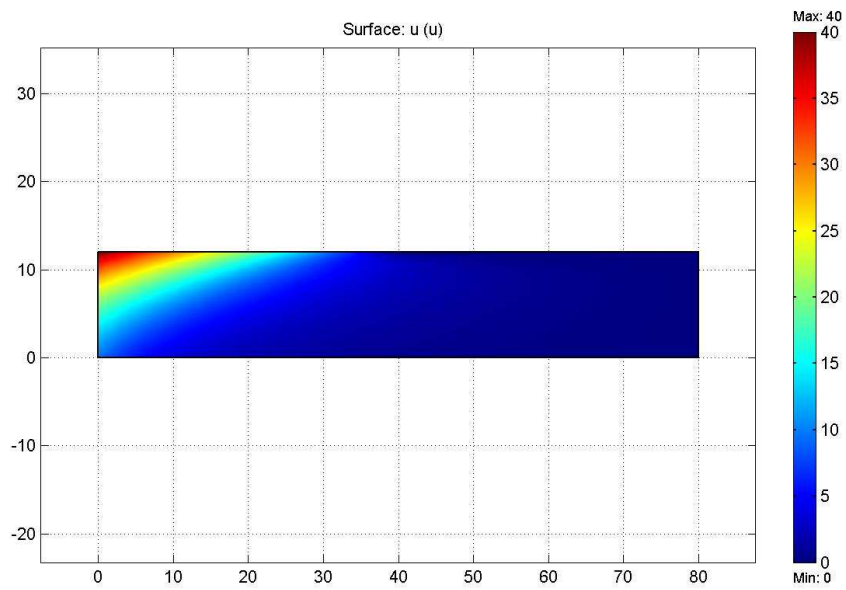


Figure 6.8: Result u of a numerical simulation using FEMLAB. The horizontal axis corresponds to x , the vertical to t .